A Search for NH₃ in the Large Magellanic Cloud

Jürgen Osterberg[1], Lister Staveley-Smith[2], Joel M. Weisberg[3],
John M. Dickey[4] and Ulrich Mebold[1]

[1] Radioastronomisches Institut der Universität Bonn, Auf dem Hügel 71,
D-53121 Bonn, Germany
[2] Australia Telescope National Facility, CSIRO, PO Box 76,
Epping, NSW 2121, Australia
[3] Department of Physics and Astronomy, Carleton College,
Northfield, MN 55057, USA
[4] Department of Astronomy, University of Minnesota, 116 Church St, SE,
Minneapolis, MN 55455, USA

Abstract: We report a search for the NH₃ $(J, K) = (1, 1)$ inversion line in the Large Magellanic Cloud (LMC) using the Parkes 64-m telescope. Candidate positions were chosen with the help of recent H I data from the Australia Telescope Compact Array and published ^{12}CO data from the Swedish–ESO Submillimetre Telescope. No detections of NH₃ in emission were found at the positions surveyed. Upper limits are approximately 25 to 74 mK.

1 Introduction

Observations of the state of the interstellar medium (ISM) in nearby galaxies allow us to probe a much greater range in physical conditions (e.g. radiation field, mass density, gas density, abundance) than is possible in our own Galaxy. The molecular phase in particular is relevant to our knowledge of processes leading to the formation of stars and stellar clusters. The most abundant observable tracer of molecular gas is ^{12}CO. However, in the case of the LMC, the nearest galaxy to us which is internally bound, the ^{12}CO emission is generally weak when compared with similar Milky Way regions (Cohen et al. 1988). The likely reason is that the strong ultraviolet radiation field in the LMC leads to greater photodissociation and lower ratios of ^{12}CO/H₂ (Israel & de Graauw 1991), H₂ being less affected by photodissociation. The actual sites of young star formation are better traced by molecules such as CS and HCO⁺ which have both been detected in the LMC. However, Booth & de Graauw (1991) remark that, because of their large dipole moment, these molecules may suffer excitation by electrons at low molecular densities when the ionisation fraction is high. Hence, it may be difficult to derive overall molecular abundances using those species. NH₃, on the other hand, has a dipole moment which is much lower than that of CS and HCO⁺, so should not suffer abnormal excitation. In our own Galaxy, NH₃ observations

have proven to be an excellent probe of dense and cold molecular cloud cores (see the review article by Ho & Townes 1983, or observational results in Ho, Martin & Barrett 1978 and Benson & Myers 1989). The richness of the NH₃ spectrum, especially of the $(J, K) = (1, 1)$ transition and its 18 hyperfine components, allows the observer to determine numerous conditions of the interstellar gas such as optical depth, excitation temperature and gas kinetic temperature. If detectable in the LMC, NH₃ would therefore prove to be a useful tool for the estimation of physical conditions in the LMC.

We have used the Parkes 64-m telescope in an attempt to search for NH₃ in a few chosen positions in the LMC. We concentrated our search near 30 Doradus, which is the largest H II region in the LMC and the most luminous and active star forming region in the Local Group. In this region, we can observe all phases of the interstellar gas: the warm diffuse gas; the cool atomic gas; the molecular clouds; and the ionised gas around newly formed stars and supernova remnants expanding into the ISM. Located south of 30 Doradus we find N 159, a bright H II region with many characteristics of the typical star-forming region.

We have also recently mapped the 21 cm H I emission with high spatial and velocity resolution around these regions with the Australia Telescope Compact Array (ATCA) and the Parkes telescope.

Table 1. Observed positions in the 30 Dor Region and around N 159

No.	Position α(J2000)	δ(J2000)	rms (mK)	Source type	Associated objects	Ref.
1	05 36 03·75	−69 30 24·02	11·9	H I condensation		4
2	05 37 23·98	−69 33 22·63	17·6	H I condensation		4
3	05 37 47·6	−69 10 21·0	23·8	H I condensation		4
4	05 39 17·0	−69 03 20·0	19·0	H I condensation		4
5	05 39 34·57	−69 45 33·6	9·21	CO condensation	LI-LMC 1501	3
6	05 39 52·1	−69 45 10	21·8	Continuum source		1
7	05 39 58·8	−70 10 57·6	24·6	CO condensation	Molecular cloud complex 35	2
8	05 40 03·9	−69 37 50·37	8·33	H I condensation		4
9	05 40 06·5	−69 44 44	11·8	IRAS point source	LI-LMC 1518	1
10	05 40 09·0	−69 44 34·0	15·9	CO condensation		1
11	05 40 37·05	−70 10 40·37	10·5	CO condensation	LI-LMC 1541	3
12	05 42 58·9	−69 45 12·5	12·5	CO condensation	LI-LMC 1609	3

[1] Hunt & Whiteoak (1994); [2] Cohen et al. (1988); [3] Israel et al. (1993); [4] Present work.

This, for the first time, gives us sufficient spatial resolution (∼10 pc) to probe dense clumps of cool neutral gas which may indicate sites of current or future star formation. The interstellar absorption survey of Dickey et al. (1994) has already shown that the cool atomic phase of the ISM near 30 Doradus is abundant in the LMC, in contrast to the relatively small number of molecular clouds detected by Cohen et al. (1988). In addition, the ESO–SEST key programme on CO in the Magellanic Clouds (Israel et al. 1993) is beginning to publish data which more directly pinpoint likely sites of dense molecular material.

We describe the NH₃ observations and data reduction in Section 2; the selection of candidate positions in Section 3; summarise the results in Section 4; and discuss the implications and future work in Section 5.

2 Observations and Data Reduction

2·1 NH₃

The observations were taken during the period 1994 February 12–21 using the Parkes telescope. The feed at the frequency of the observed NH₃ $(J, K) = (1, 1)$ transition (23·694495 GHz) only illuminates the inner 44 m of the telescope, resulting in a FWHP beamwidth of $1'\cdot4$ (20 pc at the LMC distance of 50 kpc). The efficiency of the Parkes telescope at this frequency is ∼7 Jy K⁻¹. The receiver was a single-channel maser. Owing to relatively high humidity at the time of the observations, typical system temperatures were 130 to 160 K.

The AT autocorrelator was configured to process two bands, each with 2048 channels. The first band was at the $(J, K) = (1, 1)$ transition, and the second band was used to observe the $(2, 2)$ transition at 23·722633 GHz, which is not discussed any further. The channel spacing was 7·8 kHz (0·1 km s⁻¹) with a total bandwidth of 16 MHz (202·4 km s⁻¹). At the start or end of every observing day, strong Galactic

sources were observed for calibration purposes. These sources were near the outflow region associated with the Herbig Ae star RCrA (Anglada et al. 1989) and the H II region OMC-2 in Orion (Batchelor et al. 1977). The data for each position were averaged with a weight proportional to the inverse square of the system temperature for each integration. Baselines were fitted and subtracted and a Gaussian smooth was applied resulting in a velocity resolution of 0·4 km s⁻¹. The first two positions (Nos 3 & 10 in Table 1) were observed in beam-switching mode, using a 1 Hz synchronous waveguide switch to alternate between two beams separated by $4'\cdot5$ on the sky. However, the remaining positions were observed in position-switching mode where each object was observed in a sequence consisting of 5 min on source and 5 min on a nearby 'blank-sky' region. The total integration times were typically 3 hours for each pointing.

2.2 H I

We briefly describe the λ21 cm H I data used to help choose our NH₃ target pointings. The data consist of five sets of 12-hr observations obtained in 1993 January, March, May and July with the Australia Telescope Compact Array. The uv-plane was well sampled to distances of 7 kλ (1·5 km), resulting in a synthesised FWHP beamwidth of 45″ (11 pc). We used a correlator configuration with a bandwidth of 4 MHz, divided in 1024 channels, resulting in a channel spacing of 0·8 km s⁻¹. The centre frequency was 1419 MHz, corresponding to a centre heliocentric velocity of 297 km s⁻¹. Three adjacent fields, listed in Table 2 were observed. Each field has an extent limited by the primary antenna beamwidth of 34′ (490 pc) FWHP, resulting in a combined field of approximately 1° × 1° (870×870 pc) centred approximately 12′ (170 pc) SSW of 30 Dor. The H I spectra used in this paper were extracted from the resulting data cube.

Table 2. Phase centres of fields, observed in H I with the Compact Array

Field no.	Position		Centred on
	α(J2000)	δ(J2000)	
1	05 35 27·9	−69 16 31·6	SN1987A
2	05 38 47·0	−69 05 50·1	30 Doradus
3	05 38 47·0	−69 27 49·8	Giant molecular cloud

3 The Target Positions

3.1 ^{12}CO

Searching for good candidates for high-density molecular clouds is not an easy task in the LMC. The overall CO map of Cohen et al. (1988) has a spatial resolution of 8′.8 which is too coarse to find high density clumps (nevertheless, we observed towards molecular cloud Complex 35, no. 7 in Table 1). Results from the ESO–SEST key project are still being published. The only maps published at the time of the observations were those in Booth & de Graauw (1991). Based on these maps, Hunt & Whiteoak (1994) cite coordinates of three major CO condensations in N 159, which we include in Table 1 (nos 6, 9 and 10 in Table 1). Also included is a feature which Hunt & Whiteoak discovered in their compact 4·8 GHz continuum image and the IRAS point source LI-LMC 1518. Israel et al. (1993) gave coordinates and spectra of ^{12}CO observations towards IRAS point sources, observed with SEST. Three further positions were chosen from this list: LI-LMC 1501 in N 159 which has the highest brightness temperature; LI-LMC 1609 which has a complex CO spectrum; and LI-LMC 1541 which exhibits a small line width, thus presumably tracing a very cold, dense molecular feature. In our Galaxy, the relationship between molecular material and infrared sources is striking. IRAS sources are often associated with high density clumps and thus trace the highly clumped molecular material.

3.2 H I

Existing surveys of the atomic hydrogen in the LMC were all done with the Parkes telescope and have an angular resolution of 14.′8 (e.g. Luks and Rohlfs 1992) which is far too coarse to pick out compact condensations. However, the Compact Array observations described in Section 2·2 are ideal for this purpose. To select candidates for NH$_3$ observations, we produced a map of total hydrogen column density and chose one position showing strong absorption (no. 3 in Table 1) and another position with a high column density (no. 4 in Table 1). We also produced column density maps covering more restricted (13 km s^{-1}) velocity ranges. In the first of these maps which has a mean heliocentric velocity of 212 km s^{-1} we extracted one position (no. 8 in Table 1). At a mean velocity of 278 km s^{-1} we extracted a further point (no. 2 in

Table 1). Finally, one position (no. 1 in Table 1) was extracted from a map centred at 313 km s^{-1}.

4 Results

In Figure 1 we present the observed spectra towards positions chosen on the basis of our H I data. For every NH$_3$ spectrum, we extracted the H I spectra out of our data cube at the corresponding position, except for Figure 1f where we instead extracted a CO spectrum out of the CfA 1·2 m telescope CO survey as published in Cohen et al. (1988). No NH$_3$ emission was detected with upper limits of 25 to 74 mK (3σ, where σ is listed in Column 4 of Table 1). In all of the H I spectra there are features which correspond to the two major gas components at $\sim$260 km s^{-1} and $\sim$280 km s^{-1} (Luks and Rohlfs 1992), but a wide variety of other emission and absorption features which show the complex structure of the atomic gas in this region. Figure 2 shows the NH$_3$ spectra towards the IRAS Sources LI-LMC 1501, LI-LMC 1541 and LI-LMC 1609. The ticks in these spectra indicate the velocities at which Israel et al. (1993) detected CO. Again, no NH$_3$ emission is detected.

5 Discussion

The inversion lines of NH$_3$ are generally weak due to subthermal excitation or to clumping of the molecules. We know from our own galaxy that NH$_3$ cloudlets can be quite small, of the order of 0·1 pc (C. M. Walmsley, private communication). Thus, even if the molecular cloud (as detected in ^{12}CO) is extended, the effective NH$_3$ filling fraction might be much smaller, as only a tiny part of the cloud surface area is producing emission. Consequently, with the Parkes beam of 1′·4 (20 pc) at 23 GHz, we may face severe beam dilution leading to even lower temperatures of the NH$_3$ line. For an extragalactic object, it is even more crucial to know exactly where the density peaks of the molecular material are. For defining candidate positions, we used ^{12}CO data which trace gas with a density $n(\mathrm{H}_2) \simeq 10^2$ cm^{-3}. Therefore, we may have missed the dense gas clumps. A tracer different from ^{12}CO might supply more successful candidates for a future search for NH$_3$ emission. The (1–0) transitions of HCN or HCO$^+$ have proved to be better extragalactic tracers for dense gas (Nguyen-Q-Rieu et al. 1992) as one needs densities of $n(\mathrm{H}_2) \simeq 10^4$ cm^{-3} for their excitation. Both molecules have now been detected in the LMC (Booth and Johansson 1991) and the coming millimetre data from SEST will pinpoint the density peaks in their observed fields.
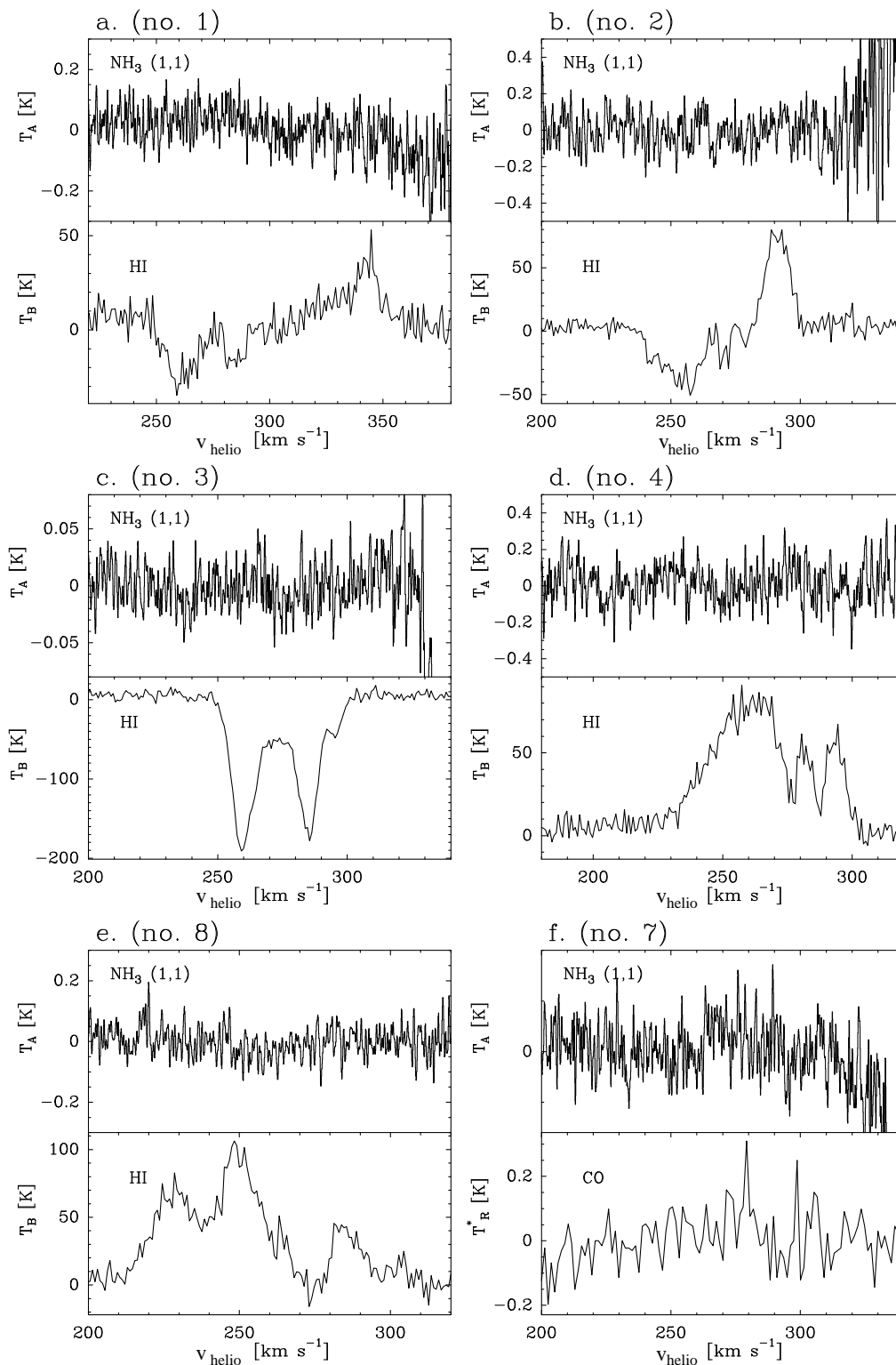
Figure 1—A comparison of our Parkes NH₃ spectra with the Compact Array H I spectra (a)–(e) and with a CO spectrum (f) observed with the CTIO 1·2 m telescope. The numbers refer to Table 1. No NH₃ emission is seen. In all of the H I spectra, features occur at typical LMC velocities, showing the two major gas components of the LMC at ~260 km s⁻¹ and ~280 km s⁻¹. Note the absorption in some of the H I spectra. The velocity scale is heliocentric.
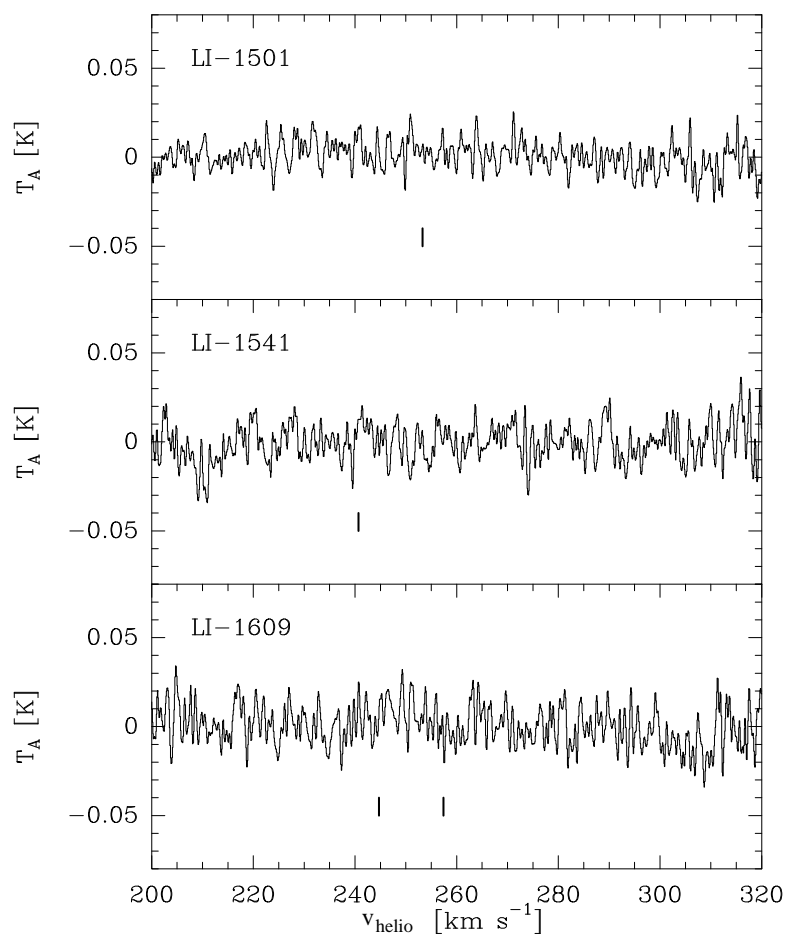
Figure 2—NH$_3$ spectra towards IRAS point sources LI-LMC 1501, LI-LMC 1541 and LI-LMC 1609. The ticks indicate the velocity of CO components detected with the SEST telescope by Israel et al. (1993).

Anglada, G., Rodriguez, L. F., Torrelles, J. M., Estalella, R., Ho, P. T. P, Canto, J., Lopez, R., & Verdes-Montenegro, L. 1989, ApJ, 341, 208

Batchelor, R. A., Gardner, F. F., Knowles, S. H., & Mebold, U. 1977, PASA, 3, 152

Benson, P. J., & Myers, P. C. 1989, ApJS, 71, 89

Booth, R. S., & de Graauw, Th. 1991, in The Magellanic Clouds, ed. R. F. Haynes & D. K. Milne, IAU Symposium No. 148, 415

Booth, R. S., & Johansson, L. E. B. 1991, in The Magellanic Clouds, ed. R. F. Haynes & D. K. Milne, IAU Symposium No. 148, 57

Cohen, R. S., Dame, T. M., Garay, G., Montani, J., Rubio, M., & Thaddeus, P. 1988, ApJ, 331, L95

Dickey, J. M., Mebold, U., Marx, M., Amy, S., Haynes, R. F., & Wilson, W. 1994, A&A, 289, 357

Ho, P. T. P., Martin, R. N., & Barrett, A. H. 1978, ApJ, 221, L117

Ho, P. T. P., & Townes, C. H. 1983, ARA&A, 21, 239

Hunt, M., & Whiteoak, J. B. 1994, PASA, 11, 68

Israel, F. P., & de Graauw, Th. 1991, in The Magellanic Clouds, ed. R. F. Haynes & D. K. Milne, IAU Symposium No. 148, 148

Israel, F. P., Johansson, L. E. B., Lequeux, J., Booth, R. S., Nyman, L. A., Crane, P., Rubio, M., de Graauw, Th., Kutner, M. L., Gredel, R., Boulanger, F., Garay, G., & Westerlund, B. 1993, A&A, 276, 25

Luks, T., & Rohlfs, K. 1992, A&A, 263, 41

Nguyen-Q-Rieu, Jackson, J. M., Henkel, C., Truong-Bach, & Mauersberger, R. 1992, ApJ, 399, 521